regular smoothing method. Figure 3 is the comparison of different preconditioning methods on FWI gradient. We can see a very strong footprint in the crossline direction due to the NAZ acquisition in Figure 3a. With a regular smoothing method, we get a velocity update as Figure 3b shows. Figure 3c shows FWI with IG preconditioning, which is free of the footprint problem and the update is blocky. By comparing Figures 3b and 3c, we note as another important feature that the IGFWI preserved the sharp boundaries of the velocity update along the major faults.

Field data example

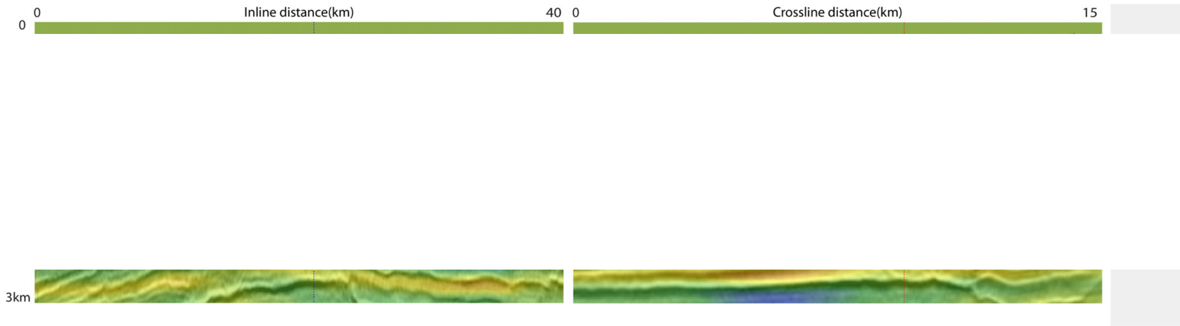

Figure 4 *FWI velocity update overlaid on migration stack image: (a) an inline section; (b) a crossline section.*

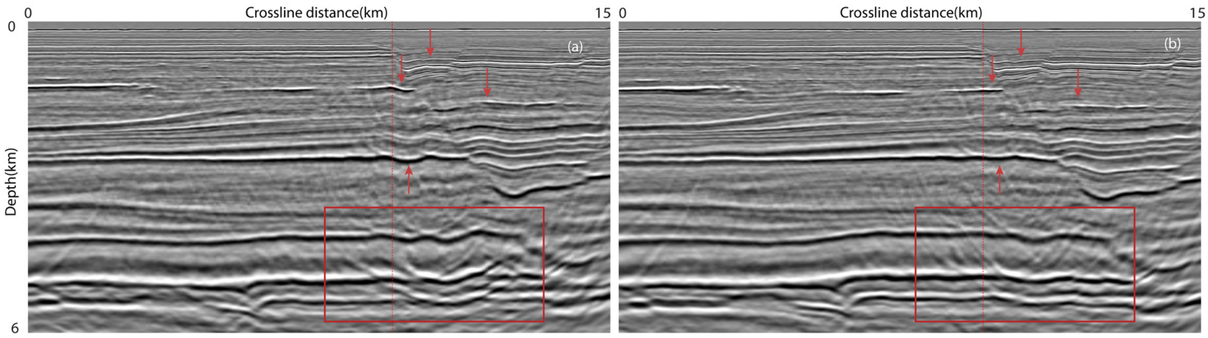

Figure 5 *Depth migration image of a crossline section: (a) migration with the initial model; (b) migration with the updated model.*

Figure 6 *Common image gathers of a crossline section: (a) CIG with the initial model; (b) CIG with the updated model.*

Our testing area in Hoop Fault Complex is 15 km by 40 km. Shot and receiver intervals are 18.75 m and 12.5 m. The streamer cable length is 6 km. The shot record length is 7.1 seconds. The sea bottom is nearly flat in the depth range of 0.43 km ~ 0.46 km. For the FWI test, the maximum frequency is up to 15 Hz. We applied some minor noise removal to the data set, but deghosting and demultiple were not applied. We begin with a Ricker wavelet for modelling and then get an updated source wavelet for inversion. We use the anisotropic VTI acoustic wave equation with a free-surface boundary condition. Anisotropic parameters 0 and were fixed and only the vertical velocity was updated. We began the DWFWI with the transmitted early arrivals to update the lowest wavenumber velocity structure. After the major update is complete, additional iterations of IGFWI were run sequentially with multi-frequency bands on top of the FWI velocity generated at the previous inversion stage. This multistage FWI gradually added high wavenumber structures to the velocity model. Because the main contribution of FWI is refraction energy and the main update is in the shallow part (up to 3 km), we run an additional tomography to update the deep portion and also to avoid few overcorrected updates from FWI.

Figure 4 is the FWI velocity update overlaid on the depth migration image. The negative update stops right at the major faults. Figure 4a and Figure 4b are an inline section and a crossline section of FWI update respectively, which are consistent with the real events. The sharp contrast on the update results from the multistage FWI update. The depth migration image with the initial model is shown in Figure 5a and the image with the updated velocity model is plotted in Figure 5b. From the comparison, we can see the sags are greatly reduced in the fault shadow area, which is more sensible geologically from an interpreter's point of view. The deep events become more continuous and focused. Figure 6 is the extracted common image gathers in this crossline section. Not only is the gather flatness improved, but also the broken gathers heal because of a more accurate model.

Conclusions

We present a robust multistage full waveform inversion methodology for practical high-resolution velocity model building. In the first stage, the newly developed DWFWI provides long-wavelength updates without cycle skipping. Then IGFWI is utilized to get a higher resolution update. IGFWI is introduced to reduce the footprint effects caused by NAZ acquisition and preserve the sharp contrast around the faults. A much higher resolution model update is obtained after this multistage FWI. We also have an additional tomography after FWI is done. Significant improvements can be seen from both the stacked image and common image gathers on the Hoop Fault Complex field data example, which proved the effectiveness of our multistage FWI workflow.

Acknowledgements

We would like to thank TGS for permission to present this work. We appreciate the helpful discussions from Simon Baldock, Bin Wang, Zhiming Li, Xuening Ma, Gary Rodriguez and Jing Chen. We thank Yang He, Rodolfo Hernandez and Guy Hilburn for tomography guidance. We also thank Connie VanSchuyver for proofreading.

References

Hale, D. [2013] Dynamic warping of seismic images, *Geophysics*, **78**(2), S105–S115.

Hart, M., Adewumi O., Lang C., Hilburn G., and Rodriguez G. [2015] High resolution velocity model building over the Hoop Fault Complex*, 85th Annual International Meeting, SEG, Expanded Abstracts*, 5189-5193.

Pratt, R. G., Shin C., and Hicks G. J. [1998] Gauss-Newton and full Newton methods in frequency-space seismic waveform inversion, *Geophysical Journal International*, **133**, 341–362.

Rodriguez, G., Lundy A., Hart M., Lang C., Cai J., Chang I. and Zhang Q. [2011] Imaging the Hoop Fault complex via horizon and fault constrained tomography: *81st Annual International meeting, SEG, Expanded Abstracts*, 4025-4029.

Virieux, J., and Operto S., [2009] An overview of full waveform inversion in exploration geophysics, *Geophysics*, **74**(6), WCC1–WCC26.